Performance Analysis of Novel Direct AccessSchemes for LEO Satellites Based IoT Network

by

ayush.dwivedi , Sai Praneeth, Sachin Chaudhari, Neeraj Varshney

Report No: IIIT/TR/2020/-1

Centre for Communications
International Institute of Information Technology
Hyderabad - 500 032, INDIA
August 2020

2020 IEEE 31st Annual International Symposium on Personal, Indoor and Mobile Radio Communications: Track 2: Networking and MAC

Performance Analysis of Novel Direct Access Schemes for LEO Satellites Based IoT Network

Ayush Kumar Dwivedi*, Sai Praneeth Chokkarapu*, Sachin Chaudhari*, Neeraj Varshney†
*International Institute of Information Technology Hyderabad, 500032 India
†Wireless Networks Division, National Institute of Standards and Technology, Gaithersburg, MD 20899 USA
ayush.dwivedi@research.iiit.ac.in, saipraneeth.c@students.iiit.ac.in, sachin.c@iiit.ac.in, neerajv@ieee.org

***Abstract*—This paper analyzes the performance of low earth orbit (LEO) satellites based internet-of-things (IoT) network, where each IoT node makes use of multiple satellites to communicate with the ground station (GS). In this work, we consider fixed and variable gain amplify-and-forward (AF) relaying protocol at each satellite, where the received signal from each IoT node is amplified before transmitting to the GS for data processing. The performance of this novel LEO satellites based direct access architecture is analyzed by deriving closed-form expressions of outage probability (OP) for two combining schemes at the GS: *(i)* selection combining *(ii)* maximal ratio combining. Both these schemes are also compared with single satellite (SS) scenario. Further, to gain more insights for diversity order and coding gain, asymptotic OP analysis at high SNR for both schemes is also performed. Finally, simulation results are presented to validate the analytical results derived and also to develop several interesting insights into the system performance.**

***Index Terms*—Satellite based IoT, LEO satellites, amplify-and-forward, outage probability**

I. Introduction

With a plan to launch 60 satellites every two weeks at 10 times lesser cost, SpaceX Starlink has proved that launching low-earth-orbit (LEO) satellites is no more a rocket science [1]. The LEO constellations like Starlink, OneWeb, Iridium, Telesat and many more under development have started a new era of affordable satellite communication. Out of the expected 20 billion connected *things* by the end of 2020, an estimated 5.3 million connections will be through satellite services [2]. Although low-power wide-area (LPWA) networks like long range (LoRa) and narrowband-IoT (NB-IoT) are designed to cater to the low-data low-power requirements of internet-of-things (IoT), these technologies fail to provide global coverage and are susceptible to natural calamities. For example, 4G wireless network currently covers 63% of world population (same expected for 5G network) but only 37% of landmass [3]. On the contrary, satellite-based access network can provide global coverage to IoT devices which are often deployed at remote locations and are dispersed over a large geographical area. In particular, large-scale LEO satellites have proved their potential in addressing coverage issues [4], [5]. For example, IoT for smart operations such as farms, oil/gas installations, electric grid etc. can benefit from satellite by extending the terrestrial coverage [6].

Integration of satellites for use in IoT networks is done in two modes [7]: *direct* access and *indirect* access. In direct access mode, the IoT devices communicate with the satellite directly, while in indirect mode, the IoT devices connect with satellite through a terrestrial LPWA gateway/relay. Such gateways have small aperture satellite terminals as well as traditional terrestrial LPWA radio modules. However, the use of indirect access is limited by the coverage of the terrestrial gateway. Investing in gateways is also not profitable in applications deployed at locations hit by disaster or locations requiring deployments for short duration. In contrast to this, direct access mode is an appealing solution for such scenarios. Thanks to the communication modules developed by companies like Iridium, Kepler and Hiber, many low powered radio modules are available in commercial market which offer direct access satellite communication from IoT nodes.

Another critical aspect of IoT applications is that, these are sensing heavy. Offloading the sensed information to a data centre is a major task. For example, use-cases like air pollution monitoring or intrusion detection involves sending status data at regular or random intervals of time. IoT devices in such scenarios do not have much computational resources to execute complex gateway selection or scheduling algorithms. For such applications, low power wide area network (LoRaWAN) protocol with star-of-stars topology, became famous in short time [8]. They make use of a gateways, which act like transparent bridges between the end-devices and the central data server. The IoT nodes broadcast their sensed information which is typically heard by multiple gateways. The central server selects information from one of the gateways and ignore the others. In a nutshell, using such an architecture, even the dumb nodes can communicate the sensed information to the data server. It is important to devise similar architectures which suit IoT requirements, but at the same time provides global coverage as well. Satellites come to rescue in this case yet again. By virtue of orbital dynamics, they can naturally support broadcast, multicast or geocast transmissions [4], where each satellite can act as a transparent bridge between the node and the central data server. This paper envisions a new architecture for direct access based LEO satellite IoT network inspired from the topology used in terrestrial LoRa networks. Constellations of LEO satellites acting as transparent relays/bridges prove to be an invaluable resource in this architecture.

In the past, many studies have been done to evaluate the performance of direct and indirect access based satellite systems. A comprehensive survey on the use of satellites for

978-1-7281-4490-0/20/$31.00 © 2020 IEEE

978-1-7281-4490-0/20/$31.00 ©2020 IEEE

IoT network is presented in [5]. The work in [9] studied a relay cooperation based hybrid satellite terrestrial network (HSTN). Authors in [10] evaluated a non-orthogonal multiple access (NOMA) assisted overlay HSTN. NOMA for LEO satellites is studied in [11]. Performance of a dual-hop satellite relaying system for multiple users is analysed in [12].

This is an introductory work and intends to establish the motivation for the idea discussed. The main contributions of this paper are described below:

- An architecture is proposed which suits sensing heavy IoT applications and also leverages the benefits of existing and upcoming mega LEO constellations. In this architecture, fixed and variable gain amplify-and-forward (AF) relaying protocol is employed at each satellite where the received signal from each IoT node is amplified before transmission to the terrestrial ground station (GS) for data processing.
- Performance of the proposed architecture is quantified in terms of OP. For this purpose, we derive closed-form analytical expressions for two different combining scheme i.e., selection combining (SC) and maximal ratio combining (MRC) at the GS.
- Asymptotic analysis of OP is done at high signal-to-noise ratio (SNR) to gain more insights into the diversity order and coding gain.

The rest of the paper is organised as following. The system model is described in Section II. This is followed by the exact and asymptotic OP analysis in Section III. Simulation results are presented in Section IV, followed by conclusions in Section V.

II. System Description

A LEO satellite based direct access architecture is considered, where a set of terrestrial IoT nodes communicate with a GS using K LEO satellites $\{S_k\}_{k=1}^{K}$, as shown in Fig. 1. Similar to the NB-IoT, where dedicated sub-carriers of 3.75 kHz or 15 kHz are utilised, it is assumed that these IoT nodes utilize separate frequency carriers such that there is no interference from adjacent nodes [13], [14]. Hence analysis is performed for a single IoT node and the same can be extended for other nodes as well. As per the proposed system model, the IoT node broadcasts its information to all the K satellites. The signal received at each of the K LEO satellites is amplified and forwarded to the GS for data-processing.

We compare the performance of this architecture in terms of OP at the GS for three different schemes:

- Scheme-1: Information is decoded at the GS using the signal received from a SS only.
- Scheme-2: Information is decoded at GS using SC scheme in which a strong signal out of K received signals from K LEO satellites is selected for decoding.
- Scheme-3: Information is decoded at the GS after coherently combining of K received signals using MRC technique.

The end-to-end communication between the IoT node and the GS takes place in two phases. In the first phase, the IoT node broadcasts its information signal to K satellites. The received signal at the kth satellite can be written as

$$y_{ns_k} = \sqrt{P_n} h_{ns_k} x_n + n_{ns_k}, \tag{1}$$

where P_n is the transit power of the IoT node, h_{ns_k} is the coefficient of the channel between the IoT node and the kth satellite, x_n is the unit energy information signal and n_{ns_k} the additive noise modeled as independent and identically distributed (i.i.d.) symmetric complex Gaussian with mean zero and variance σ^2.

In the second phase, each satellite relays the signal received from IoT node to the GS by employing AF relaying scheme. Therefore, the signal received at the GS from the kth satellite can be written as

$$y_{s_k g} = \sqrt{P_{s_k}} h_{s_k g} \mathbb{G} (\sqrt{P_n} h_{ns_k} x_n + n_{ns_k}) + n_{s_k g}, \tag{2}$$

where P_{s_k} is the transit power of the kth satellite, $h_{s_k g}$ is the coefficient of the channel between the kth satellite and the GS, $\mathbb{G}$ is the AF gain factor and $n_{s_k g}$ is the additive white Gaussian noise (AWGN) noise at the GS receiver. Note that all the channel coefficients corresponding to node-satellite and satellite-GS links i.e., h_{ns_k} and $h_{s_k g}, \forall k$, are assumed to follow shadowed-Rician (SR) distribution. The SR fading model is best known for characterizing communication links which suffer from LoS shadowing and small scale fading [15]. It is a more generalized form of Rician fading model where the amplitude of the LoS component follows Nakagami-m fading. Moreover, this model is widely accepted for characterizing satellite channels and fits the experimental data very well.

Using (1), the instantaneous SNR at the kth satellite for the node-satellite link is given by $\Lambda_{ns_k} = P_n |h_{ns_k}|^2 / \sigma^2 = \eta_n |h_{ns_k}|^2$, where $\eta_n = \frac{P_n}{\sigma^2}$. Further, under scheme-1 (SS), the instantaneous SNR at the GS corresponding to the transmission by the kth satellite can be derived as

$$\Lambda_{\text{GS}}^{\text{SS}} = \frac{\Lambda_{s_k g} \, \Lambda_{ns_k}}{\Lambda_{s_k g} + C}, \tag{3}$$

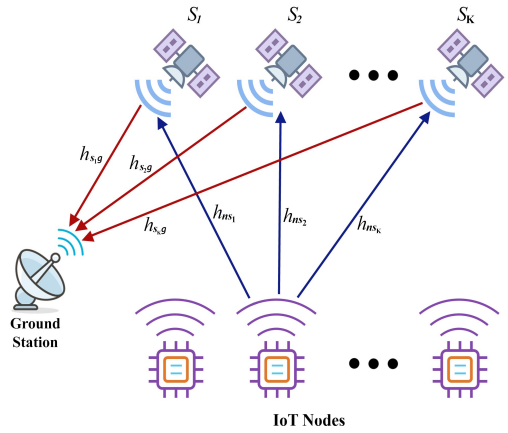

Fig. 1. Schematic diagram of the proposed LEO satellite based direct access network where multiple IoT nodes communicate to GS using K LEO satellites, which are in LoS

where $\Lambda_{s_kg} = \eta_{s_k}|h_{s_kg}|^2$, $\eta_{s_k} = P_{s_k}/\sigma^2$ and $C = 1/\mathbb{G}^2\sigma^2$. Similar to [16], the AF gain factor $\mathbb{G}$ is defined as

$$\mathbb{G} = \left(P_n|h_{ns_k}|^2 + \sigma^2\right)^{-\frac{1}{2}}. \tag{4}$$

In (3), the term C can be simplified to $1+\Lambda_{ns_k}$ or $1+\mathbb{E}[\Lambda_{ns_k}]$ depending upon the choice of variable gain or fixed gain relaying [16]. Similarly, the instantaneous SNRs at the GS under scheme-2 (SC) and scheme-3 (MRC) are derived as

$$\Lambda_{\text{GS}}^{\text{SC}} = \max_k \left(\frac{\Lambda_{s_kg}\ \Lambda_{ns_k}}{\Lambda_{s_kg} + C}\right), \tag{5}$$

$$\Lambda_{\text{GS}}^{\text{MRC}} = \frac{\sum_{k=1}^{K}(\Lambda_{s_kg})\ \sum_{k=1}^{K}(\Lambda_{ns_k})}{\sum_{k=1}^{K}(\Lambda_{s_kg}) + C_m}, \tag{6}$$

where C_m is defined as $C_m = 1/(\sigma^2 \sum_{k=1}^{K} \mathbb{G}^2)$.

A. Statistical characteristics of shadowed-Rician channel

The probability density function (PDF) and cumulative distribution function (CDF) of $\Lambda_i = \eta_i|h_i|^2$, $i \in \{ns_k, s_kg\}$ and $k \in \{1, 2, \ldots, K\}$ are given, respectively in [10] by

$$f_{\Lambda_i(x)} = \alpha_i \sum_{\kappa=0}^{m_i-1} \frac{\zeta(\kappa)}{\eta_i^{\kappa+1}} x^{\kappa} e^{-\left(\frac{\beta_i-\delta_i}{\eta_i}\right)x}, \tag{7}$$

$$F_{\Lambda_i(x)} = 1 - \alpha_i \sum_{\kappa=0}^{m_i-1} \frac{\zeta(\kappa)}{\eta_i^{\kappa+1}} \sum_{p=0}^{\kappa} \frac{\kappa!}{p!} \left(\frac{\beta_i-\delta_i}{\eta_i}\right)^{-(\kappa+1-p)} \times x^p e^{-\left(\frac{\beta_i-\delta_i}{\eta_i}\right)x}, \tag{8}$$

where $\alpha_i = ((2b_im_i)/(2b_im_i+\Omega_i))^{m_i}/2b_i$, $\beta_i = 1/2b_i$, $\delta_i = \Omega_i/(2b_i)(2b_im_i + \Omega_i)$ and $\zeta(\kappa) = (-1)^{\kappa}(1-m_i)_{\kappa}\delta_i^{\kappa}/(\kappa!)^2$ with $(\cdot)_{\kappa}$ being the Pochhammer symbol [17]. Here $2b_i$ denotes the average power of the multipath component, Ω_i is the average power of the LoS component

III. Outage Performance of LEO satellite based direct access IoT network

In this section, the performance of the proposed architecture is analyzed. For this purpose, closed-form expressions for OP in all the three schemes are derived.

A. Outage Probability Analysis

1) Scheme-1 (SS): The OP at the GS in the case of single satellite can be evaluated as

$$\begin{aligned} P_{\text{out}}^{\text{SS}}(R) &= \Pr\left[\frac{1}{2}\log_2(1+\Lambda_{\text{GS}}^{\text{SS}}) \le R\right] \\ &= \Pr\left[\frac{\Lambda_{sg}\ \Lambda_{ns}}{\Lambda_{sg}+C} \le \gamma_{\text{th}}\right], \end{aligned} \tag{9}$$

where R is the target rate and $\gamma_{\text{th}} \triangleq 2^{2R} - 1$. We can reformulate (9) under variable gain relaying as

$$P_{\text{out}}^{\text{SS}}(R) = \Pr\left[(\Lambda_{sg} - \gamma_{\text{th}})(\Lambda_{ns} - \gamma_{\text{th}}) \le \gamma_{\text{th}}^2 + \gamma_{\text{th}}\right]. \tag{10}$$

Further, using (7), the above expression is mathematically intractable and difficult to solve in closed-form. Hence, we employ an M-step-staircase approximation approach as in [18]. Using this approach, the closed-form expression for $P_{\text{out}}^{\text{SS}}(R)$ is derived as (11), where $\Upsilon = \gamma_{\text{th}}^2 + \gamma_{\text{th}}$. The detailed proof of (11) is given in Appendix A.

2) Scheme-2 (SC): The OP at the GS in the case of the SC can be evaluated as

$$P_{\text{out}}^{\text{SC}}(R) = \Pr\left[\max_k \left(\frac{\Lambda_{s_kg}\ \Lambda_{ns_k}}{\Lambda_{s_kg}+C}\right) \le \gamma_{\text{th}}\right]. \tag{12}$$

Further, following the similar analysis as done in the case of scheme-1, the closed form expression for SC under variable gain AF relaying can be derived as

$$P_{\text{out}}^{\text{SC}} = \prod_{k=1}^{K} P_{\text{out,k}}^{\text{SS}}(R), \tag{13}$$

where $P_{\text{out,k}}^{\text{SS}}(R)$ is given in (11).

3) Scheme-3 (MRC): Using (6), the OP in the case of MRC is given by

$$P_{\text{out}}^{\text{MRC}}(R) = \Pr\left[\frac{\Delta_{sg}\ \Delta_{ns}}{\Delta_{sg}+C_m} \le \gamma_{\text{th}}\right], \tag{14}$$

where Δ_{sg} and Δ_{ns} are defined as $\Delta_{sg} \triangleq \sum_{k=1}^{K}(\Lambda_{s_kg})$ and $\Delta_{ns} \triangleq \sum_{k=1}^{K}(\Lambda_{ns_k})$. The CDF of $\Delta_i, i \in \{sg, ns\}$ is given in Appendix B. Due to analytical tractability, we reformulate (14) under fixed gain relaying as

$$P_{\text{out}}^{\text{MRC}}(R) = \Pr\left[(\Delta_{sg})(\Delta_{ns} - \gamma_{\text{th}}) \le C_m\gamma_{\text{th}}\right], \tag{15}$$

where C_m is given as $\left[\sum_{k=1}^{K} 1/(1+\mathbb{E}\left[\Lambda_{ns_k}\right])\right]^{-1}$. It is worth-mentioning that $\mathbb{E}\left[\Lambda_{ns_k}\right]$ can be derived analytically by calculating the expectation over (7). The derived simplified expression for $\mathbb{E}\left[\Lambda_i\right]$ is given by

$$\mathbb{E}\left[\Lambda_i\right] = \alpha_i \sum_{\kappa=0}^{m_i-1} \zeta(\kappa)\eta_i \frac{\Gamma(\kappa+2)}{(\beta_i-\delta_i)^{\kappa+2}}. \tag{16}$$

Further, after applying the M-step-staircase approximation for (15), the closed-form expression for OP in case of MRC can be derived as (17). The proof can be carried out by following the similar steps as shown in Appendix A.

B. Asymptotic Outage Probability Analysis

In this section, we provide the asymptotic OP analysis under high SNR assumption. This will help us to gain more insight about the network in terms of diversity order that it can achieve.

At high SNR i.e., $\eta_n, \eta_{s_k} \to \infty$, the CDFs used in (11) and (17) can be approximated respectively as in [12] by

$$F_{\Lambda_i}^{\infty}(x) \approx \frac{\alpha_i}{\eta_i}x, \quad \text{and} \quad F_{\Delta_i}^{\infty}(x) \approx \frac{\alpha_i^K}{\eta_i^K\Gamma(K+1)}x^K. \tag{18}$$

The total transmit power of the system, P_t can be written as $P_t = P_n + \sum_{k=1}^{K} P_{s_k}$. Considering equal power allocation, the asymptotic OP for scheme-2 and scheme-3 can be derived respectively, as

$$P_{\text{out}}^{\text{SC},\infty} = \left(\frac{\gamma_{\text{th}}}{\eta}\prod_{k=1}^{K}\sqrt[K]{(\alpha_{s_kg}+\alpha_{ns_k})}\right)^K + O\left(\frac{1}{\eta^K}\right), \tag{19}$$

$$P_{\text{out}}^{\text{MRC},\infty} = \left(\frac{\gamma_{\text{th}}\alpha_{ns}}{\sqrt[K]{\Gamma(K+1)}\eta}\right)^K + O\left(\frac{1}{\eta^K}\right), \tag{20}$$

$$P_{\text{out}}^{\text{SS}}(R) = F_{\Lambda_{sg}}(\gamma_{\text{th}}) + \left\{F_{\Lambda_{ns}}(\gamma_{\text{th}}) \times \left[1 - F_{\Lambda_{sg}}(\gamma_{\text{th}})\right]\right\} + \left\{\left[F_{\Lambda_{sg}}(\sqrt{\Upsilon} + \gamma_{\text{th}}) - F_{\Lambda_{sg}}(\gamma_{\text{th}})\right] \times \left[F_{\Lambda_{ns}}(\sqrt{\Upsilon} + \gamma_{\text{th}}) - F_{\Lambda_{ns}}(\gamma_{\text{th}})\right]\right\}$$
$$+ \sum_{i=1}^{M} \left\{\left[F_{\Lambda_{sg}}\left(\frac{\Upsilon}{\sqrt{\Upsilon} + \frac{i-1}{M}L} + \gamma_{\text{th}}\right) - F_{\Lambda_{sg}}(\gamma_{\text{th}})\right] \times \left[F_{\Lambda_{ns}}\left(\sqrt{\Upsilon} + \gamma_{\text{th}} + \frac{iL}{M}\right) - F_{\Lambda_{ns}}\left(\sqrt{\Upsilon} + \gamma_{\text{th}} + \frac{(i-1)L}{M}\right)\right]\right\}$$
$$+ \sum_{i=1}^{M} \left\{\left[F_{\Lambda_{ns}}\left(\frac{\Upsilon}{\sqrt{\Upsilon} + \frac{i-1}{M}L} + \gamma_{\text{th}}\right) - F_{\Lambda_{ns}}(\gamma_{\text{th}})\right] \times \left[F_{\Lambda_{sg}}\left(\sqrt{\Upsilon} + \gamma_{\text{th}} + \frac{iL}{M}\right) - F_{\Lambda_{sg}}\left(\sqrt{\Upsilon} + \gamma_{\text{th}} + \frac{(i-1)L}{M}\right)\right]\right\}, \quad (11)$$

$$P_{\text{out}}^{\text{MRC}}(R) = F_{\Delta_{ns}}(\gamma_{\text{th}}) + \left\{F_{\Delta_{sg}}(\sqrt{C_m\gamma_{\text{th}}}) \times \left[F_{\Delta_{ns}}\left(\sqrt{C_m\gamma_{\text{th}}} + \gamma_{\text{th}}\right) - F_{\Delta_{ns}}(\gamma_{\text{th}})\right]\right\}$$
$$+ \sum_{i=1}^{M} \left\{F_{\Delta_{sg}}\left(\frac{C_m\gamma_{\text{th}}}{\sqrt{C_m\gamma_{\text{th}}} + \frac{i-1}{M}L}\right) \times \left[F_{\Delta_{ns}}\left(\sqrt{C_m\gamma_{\text{th}}} + \gamma_{\text{th}} + \frac{i}{M}L\right) - F_{\Delta_{ns}}\left(\sqrt{C_m\gamma_{\text{th}}} + \gamma_{\text{th}} + \frac{i-1}{M}L\right)\right]\right\}$$
$$+ \sum_{i=1}^{M} \left\{\left[F_{\Delta_{sg}}\left(\sqrt{C_m\gamma_{\text{th}}} + \frac{i}{M}L\right) - F_{\Delta_{sg}}\left(\sqrt{C_m\gamma_{\text{th}}} + \frac{i-1}{M}L\right)\right] \times \left[F_{\Delta_{ns}}\left(\frac{C_m\gamma_{\text{th}}}{\sqrt{C_m\gamma_{\text{th}}} + \frac{i-1}{M}L} + \gamma_{\text{th}}\right) - F_{\Delta_{ns}}(\gamma_{\text{th}})\right]\right\}, \quad (17)$$

where $O(\cdot)$ stands for higher order terms. The OP at high SNR can be approximated as

$$P_{\text{out}}^{\infty} = (G_c\eta)^{-d} + O(\eta^{-d}), \quad (21)$$

where G_c and d denote the coding gain and the diversity order, respectively. Hence, by comparing (19), (20) and (21), the diversity order of the system for both scheme-2 and scheme-3 can be seen as K. Moreover, the respective coding gains are

$$G_c^{\text{SC}} = \left(\gamma_{\text{th}} \prod_{k=1}^{K} \sqrt[K]{(\alpha_{s_kg} + \alpha_{ns_k})}\right)^{-1}, \quad (22)$$

$$G_c^{\text{MRC}} = \sqrt[K]{\Gamma(K+1)}(\gamma_{\text{th}}\alpha_{ns})^{-1}. \quad (23)$$

IV. Simulation Results

This section presents simulation results to validate the derived analytical results of this work and to develop several important insights into the system performance. For simulation purpose in MATLAB, we consider the following four possible shadowing conditions for all the three schemes:

(a) H-H: each h_{ns_k} and h_{s_kg} under heavy shadowing (H)
(b) H-A: each h_{ns_k} under heavy shadowing (H) and each h_{s_kg} under average shadowing (A)
(c) A-H: each h_{ns_k} under average shadowing (A), each h_{s_kg} under heavy shadowing (H)
(d) A-A: each h_{ns_k} and h_{s_kg} under average shadowing (A)

The SR fading parameters (m, b, Ω) under heavy and average shadowing conditions are considered to be $(2, 0.063, 0.0005)$ and $(5, 0.251, 0.279)$, respectively [19]. We set the target rate $R = 0.5$ so that $\gamma_{\text{th}} = 1$ [10]. For step-staircase approximation, we set $M = 50$ and $L = 15\gamma_{\text{th}}$. For simplicity in simulation, we consider equal power allocation with $\eta_n = \eta_{s_k} = \eta$ as the transmit SNR.

Further, to be able to identify the range of SNR values which are feasible for proposed IoT network, we performed the link budget analysis as given in [20]. For link budget, we consider a LEO satellite at an altitude of 800 km, uplink central frequency of 950 MHz, satellite elevation angle of 30°, 3GPP Class 3 IoT node transmit equivalent isotropically radiated power (EIRP) of 23 dBm [21], and sub-carrier bandwidths of 3.7 kHz , 15 kHz, 45 kHz, 90 kHz and 180 kHz. For LEO satellite receiver antenna gain-to-noise-temperature (G/T) varying from -25 dBi/K to -6 dBi/K, SNR in the approximate range of -9 dB to 20 dB are found feasible for our network. Thus, this SNR range is considered for simulations under all the four possible channel conditions.

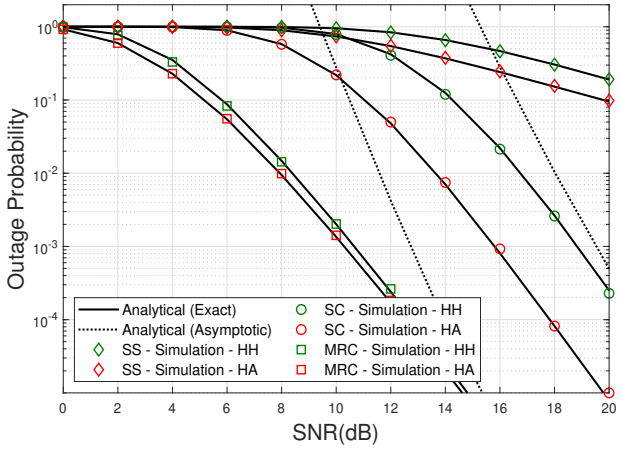

Fig. 2. OP versus SNR curves for all three schemes under H-H and H-A conditions using $\gamma_{\text{th}} = 1, M = 50, L = 15 \times \gamma_{\text{th}}$, and $K = 5$.

Fig. 2 shows the outage performance of the system against SNR by considering five LEO satellites in LoS. This figure considers shadowing conditions (a) and (b). We are using AF relaying where the signal is amplified without decoding as opposed to decode-and-forward (DF) where the effect of shadowing can be un-done by decoding at the relay. As a result, the effect of node-satellite link shadowing is clearly visible on the performance. In this figure, node-satellite link is under heavy shadowing, consequently the OP is significantly high for SNR less than 0 dB. Hence the OP curves are plotted for SNR ranging from 0 dB to 20 dB in this figure to validate our closed form expressions. It can be seen that the MRC and SC schemes outperforms the SS scheme. This proves the superiority of the proposed architecture and establishes how it is able to leverage the benefits of multiple satellites available as part of mega LEO constellations. One can also observe that the MRC performs significantly better than the

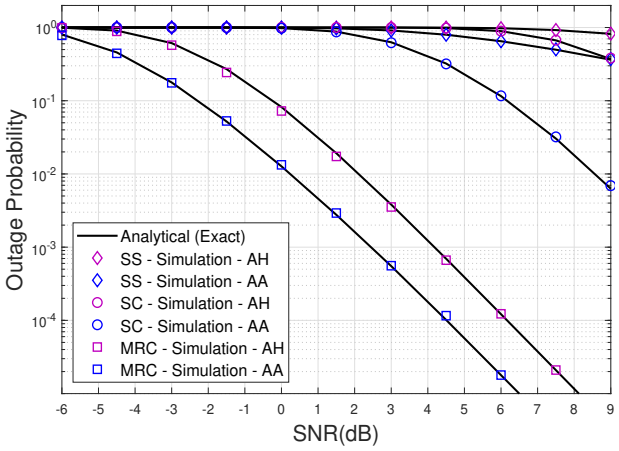

Fig. 3. OP versus SNR curves for all three schemes under A-H and A-A conditions using $\gamma_{\text{th}} = 1, M = 50, L = 15 \times \gamma_{\text{th}}$, and $K = 5$.

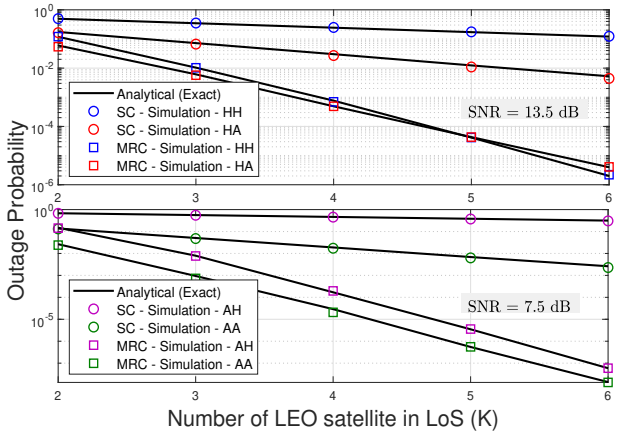

Fig. 4. OP versus number of satellites in LoS (K) for scheme-2 and scheme-3 using $\gamma_{\text{th}} = 1, M = 50, L = 15 \times \gamma_{\text{th}}$ and $\eta = 13.5$dB for H-A, H-H conditions and $\eta = 7.5$dB for A-H, A-A conditions.

SC. Approximately 6dB higher SNR is required in case of the SC when compared to the MRC, for an OP of 10^{-2}. Another key observation is that, in the case of SC, approximately 3dB higher SNR is required when the satellite-GS channel changes from average to heavy. Whereas such drastic effect of change in channel shadowing on outage performance is not seen in the case of MRC. Therefore, MRC proves to be much more robust towards change in shadowing conditions of satellite-GS channel. The asymptotic curves approach the exact analytical curves sharply, thus validating the correctness of the derived formulae. It is also observed that the slope of OP curves for SC and MRC are similar towards higher SNR. This is indicative of the fact that diversity order depends on the number of satellites in LoS.

Fig. 3 shows the outage performance for shadowing conditions (c) and (d). Here the node-satellite channel is considered to be under average shadowing. Consequently as the result of AF relaying, the OP is significantly low for SNR greater than 9 dB. Hence OP curves are plotted for SNR ranging from -6 dB to 9 dB in this figure to validate our closed form expressions. Observations similar to Fig. 2 can be made regarding the better performance of the MRC when compared to the SC. Although the MRC still proves to be more robust than the SC towards change in satellite-GS link shadowing conditions, the difference in SNR is high compared to Fig. 2.

To gain more insights about the architecture, we also plot the OP versus number of satellites (K) in Fig.4. A comparison between three famous commercial LEO constellations (SpaceX-Starlink, OneWeb, Telesat) in terms of possible number of satellites in LoS is given in [22]. According to that, for latitudes where majority of world's population is located, 2 to 30 LEO satellites can be in LoS based on location of user equipment. Hence we simulate for K in the range of 2 to 6. It can be seen from the plot that the system performance can be significantly enhanced by increasing K. This means that the performance of proposed architecture would increase as and when new constellations or satellites are added in network. It is also observed that system utilizing the MRC benefits more when compared to the SC with increase in number of satellites under all channel conditions.

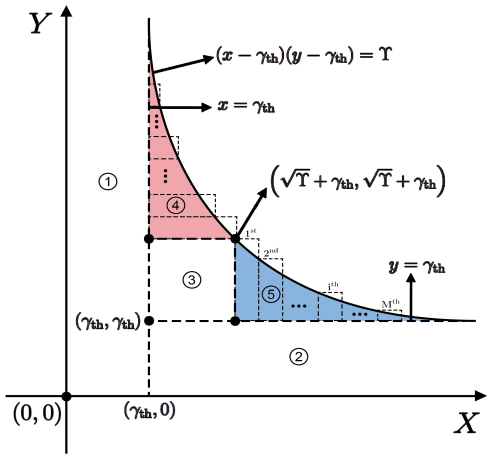

Fig. 5. Regions of integration for calculating exact OP expression in scheme-1. Regions 1, 2 and 3 are calculated by direct integration, step staircase approximation is applied for only regions 4 and 5.

V. Conclusion

With the advent of mega LEO constellations and direct access LEO radio modules for IoT, satellite based IoT networks have become a feasible choice for mass deployments. Performance analysis of a novel architecture for IoT nodes which do not have much computational resources is done. It is found that both the SC and the MRC schemes have the same diversity gain but different coding gains. This makes the MRC scheme perform better than SC scheme. The proposed architecture suits present era of burgeoning number of LEO satellite constellations and makes clever use of all the available satellite resources. In future, we intend to study this architecture by incorporating aspects like optimum power allocation between IoT node and satellite terminals and effect of interference form nearby satellites and other radio devices.

Appendix A
Derivation of (11)

To obtain the closed-form expression, we have to solve an equation of the form

$$P_{\text{out}} = \Pr\left[(X - \gamma_{\text{th}})(Y - \gamma_{\text{th}}) \leq \Upsilon\right] \tag{24}$$

where X, Y and Υ are defined from (10) as $X = \Lambda_{s_k g}$, $Y = \Lambda_{n s_k}$ and $\Upsilon = \gamma_{\text{th}}^2 + \gamma_{\text{th}}$, respectively. To solve (24), we can approximate the integral in five regions as shown in Fig. 5. For regions 4 and 5, following the process given in [18], we divide the integral region into M vertical blocks. We divide region 4 into M blocks from $Y = \sqrt{\Upsilon} + \gamma_{\text{th}}$ to $Y = \sqrt{\Upsilon} + \gamma_{\text{th}} + (L \times \gamma_{\text{th}})$, where L is the depth of integration. Similarly we divide region 5 into M blocks from $X = \sqrt{\Upsilon} + \gamma_{\text{th}}$ to $X = \sqrt{\Upsilon} + \gamma_{\text{th}} + (L \times \gamma_{\text{th}})$. It is also important to note that, since X and Y are independent random variables, the integral values for regions R_1 to R_3, and ith block of R_4 and R_5 can be evaluated as

$$R_1 = \int_{y=0}^{\infty} \int_{x=0}^{\gamma_{\text{th}}} f_{X,Y}(x,y) dx dy = F_X(\gamma_{\text{th}}). \tag{25}$$

$$R_2 = \int_{y=0}^{\gamma_{\text{th}}} \int_{x=\gamma_{\text{th}}}^{\infty} f_{X,Y}(x,y) dx dy = F_Y(\gamma_{\text{th}}) \left[1 - F_X(\gamma_{\text{th}})\right]. \tag{26}$$

$$\begin{aligned} R_3 &= \int_{y=\gamma_{\text{th}}}^{\sqrt{\Upsilon}+\gamma_{\text{th}}} \int_{x=\gamma_{\text{th}}}^{\sqrt{\Upsilon}+\gamma_{\text{th}}} f_{X,Y}(x,y)\ dx dy \\ &= \left[F_X(\sqrt{\Upsilon}+\gamma_{\text{th}}) - F_X(\gamma_{\text{th}})\right]\left[F_Y(\sqrt{\Upsilon}+\gamma_{\text{th}}) - F_Y(\gamma_{\text{th}})\right]. \end{aligned} \tag{27}$$

$$\begin{aligned} R_4^i &= \int_{y=\sqrt{\Upsilon}+\gamma_{\text{th}}+\frac{i-1}{M}L}^{\sqrt{\Upsilon}+\gamma_{\text{th}}+\frac{i}{M}L} \int_{x=\gamma_{\text{th}}}^{\frac{\Upsilon}{\sqrt{\Upsilon}+\frac{i-1}{M}L}+\gamma_{\text{th}}} f_{X,Y}(x,y)\ dx dy \\ &= \left[F_X\left(\frac{\Upsilon}{\sqrt{\Upsilon}+\frac{i-1}{M}L}+\gamma_{\text{th}}\right) - F_X(\gamma_{\text{th}})\right] \\ &\quad \times \left[F_Y\left(\sqrt{\Upsilon}+\gamma_{\text{th}}+\frac{iL}{M}\right) - F_Y\left(\sqrt{\Upsilon}+\gamma_{\text{th}}+\frac{(i-1)L}{M}\right)\right]. \end{aligned} \tag{28}$$

$$\begin{aligned} R_5^i &= \int_{y=\gamma_{\text{th}}}^{\frac{\Upsilon}{\sqrt{\Upsilon}+\frac{i-1}{M}L}+\gamma_{\text{th}}} \int_{x=\sqrt{\Upsilon}+\gamma_{\text{th}}+\frac{i-1}{M}L}^{\sqrt{\Upsilon}+\gamma_{\text{th}}+\frac{i}{M}L} f_{X,Y}(x,y)\ dx dy \\ &= \left[F_Y\left(\frac{\Upsilon}{\sqrt{\Upsilon}+\frac{i-1}{M}L}+\gamma_{\text{th}}\right) - F_Y(\gamma_{\text{th}})\right] \\ &\quad \times \left[F_X\left(\sqrt{\Upsilon}+\gamma_{\text{th}}+\frac{iL}{M}\right) - F_X\left(\sqrt{\Upsilon}+\gamma_{\text{th}}+\frac{(i-1)L}{M}\right)\right]. \end{aligned} \tag{29}$$

Finally, the final closed-form expression for OP is given by

$$P_{\text{out}} = R_1 + R_2 + R_3 + \sum_{i=1}^{M} R_4^i + \sum_{i=1}^{M} R_5^i. \tag{30}$$

APPENDIX B
CDF OF SUM OF SR RANDOM VARIABLES

The CDF of $\Delta_i, i \in \{sg, ns\}$ which is the sum of K SR random variables, is given by [23]

$$\begin{aligned} F_{\Delta_i}(x) = \alpha_i^K \sum_{l=0}^{c} \binom{c}{l} \beta_i^{c-l} (\mathcal{G}(x,l,d,\eta) \\ + \epsilon \delta_i \mathcal{G}(x,l,d+1,\eta)), \end{aligned} \tag{31}$$

where $c = (d-K)^+, \epsilon = m_i K - d, d = \max\{K, \lfloor m_i K \rfloor\}$. $\mathcal{G}(x,l,d,\eta)$ is given as

$$\begin{aligned} \mathcal{G}(x,l,d,\eta) = \frac{(\beta_i - \delta_i)^{\frac{l-d-1}{2}}}{\eta^{\frac{d-l-1}{2}} \Gamma(d-l+1)} x^{\frac{d-l-1}{2}} e^{-\frac{\beta_i - \delta_i}{2\eta} x} \\ \times M_{\frac{d+l-1}{2}, \frac{d-l}{2}}\left(\frac{\beta_i - \delta_i}{\eta} x\right), \end{aligned} \tag{32}$$

where $M_{\mu,\nu}(\cdot)$ represents the Whittaker function [17].

REFERENCES

[1] Jonathan O'Callaghan, "Spacex launches 60 starlink mega constellation satellites into orbit on starlink-1 mission," *Forbes Media*, Nov 11, 2019.

[2] "M2M and IoT via satellite," *Northern Sky Research - 10th edition*, 2019.

[3] N. Chuberre, "5G satellite (standardization activities in 3GPP, target solutions for remote and rural areas)," *India-EU Partnership Project on Collaboration for ICT Standardisation*, 2019.

[4] N. Accettura J. Fraire, S. Céspedes, "Direct-to-satellite IoT - a survey of the state of the art and future research perspectives: Backhauling the IoT through LEO satellites," *ADHOC-NOW: Ad-Hoc, Mobile, and Wireless Networks*, pp. 241–258, 2019.

[5] Z. Qu, G. Zhang, H. Cao, and J. Xie, "LEO satellite constellation for internet of things," *IEEE Access*, vol. 5, pp. 18391–18401, 2017.

[6] R. G. Gopal and N. B. Ammar, "Framework for unifying 5G and next generation satellite communications," *IEEE Network*, vol. 32, no. 5, pp. 16–24, 2018.

[7] F. Chiti, R. Fantacci, and L. Pierucci, "Energy efficient communications for reliable IoT multicast 5G/satellite services," *Future Internet*, 2019.

[8] I. Lysogor, L. Voskov, et al., "Study of data transfer in a heterogeneous LoRa-satellite network for the internet of remote things," *MDPI Sensors*, 2019.

[9] S. Sreng, B. Escrig, and M. Boucheret, "Exact outage probability of a hybrid satellite terrestrial cooperative system with best relay selection," *IEEE International Conference on Communications (ICC)*, pp. 4520–4524, 2013.

[10] V. Singh, P. K. Upadhyay, and M. Lin, "On the performance of noma-assisted overlay multiuser cognitive satellite-terrestrial networks," *IEEE Wireless Communications Letters*, pp. 1–1, 2020.

[11] Z. Gao, A. Liu, and X. Liang, "The performance analysis of downlink NOMA in LEO satellite communication system," *IEEE Access*, vol. 8, pp. 93723–93732, 2020.

[12] Wu Xuewen, Lin Min, et al., "Performance analysis of multiuser dual-hop satellite relaying systems," *EURASIP Journal on Wireless Communications and Networking*, pp. 1687–1499, 2019.

[13] S. Cluzel, L. Franck, et al., "3GPP NB-IoT coverage extension using LEO satellites," *IEEE 87th Vehicular Technology Conference (VTC Spring)*, pp. 1–5, 2018.

[14] T. Ferrer and S. Céspedes, "Review and evaluation of MAC protocols for satellite IoT systems using nanosatellites," *MDPI Sensors*, 2019.

[15] A. Abdi, W. C. Lau, M. Alouini, and M. Kaveh, "A new simple model for land mobile satellite channels: first- and second-order statistics," *IEEE Transactions on Wireless Communications*, vol. 2, no. 3, pp. 519–528, 2003.

[16] P. K. Upadhyay and P. K. Sharma, "Max-max user-relay selection scheme in multiuser and multirelay hybrid satellite-terrestrial relay systems," *IEEE Communications Letters*, vol. 20, no. 2, pp. 268–271, 2016.

[17] I.S. Gradshteyn and I.M. Ryzhik, "Tables of integrals, series and products," *New York: Academic Press*, 2000.

[18] C. Zhang, J. Ge, J. Li, Y. Rui, and M. Guizani, "A unified approach for calculating the outage performance of two-way af relaying over fading channels," *IEEE Transactions on Vehicular Technology*, vol. 64, no. 3, pp. 1218–1229, 2015.

[19] N. I. Miridakis, D. D. Vergados, and A. Michalas, "Dual-hop communication over a satellite relay and shadowed rician channels," *IEEE Transactions on Vehicular Technology*, vol. 64, no. 9, pp. 4031–4040, 2015.

[20] O. Kodheli, N. Maturo, et al., "Link budget analysis for satellite-based narrowband IoT systems," *International Conference on Ad Hoc Networks and Wireless*, 2019.

[21] Technical Specification (TS) 36.101, "Evolved universal terrestrial radio access; user equipment radio transmission and reception (release 14)," *3rd Generation Partnership Project (3GPP)*, 2017.

[22] I. Portillo, B. G. Cameron, and E. F. Crawley, "A technical comparison of three low earth orbit satellite constellation systems to provide global broadband," *Acta Astronautica*, vol. 159, pp. 123 – 135, 2019.

[23] M. R. Bhatnagar and A. M.K., "On the closed-form performance analysis of maximal ratio combining in shadowed-rician fading lms channels," *IEEE Communications Letters*, vol. 18, no. 1, pp. 54–57, 2014.